Case Studies in Construction Materials 17 (2022) e01580

Contents lists available at ScienceDirect

Case Studies in Construction Materials

journal homepage: www.elsevier.com/locate/cscm

Evaluation and calibration of dynamic modulus prediction models of asphalt mixtures for hot climates: Qatar as a case study

Ahmad Al-Tawalbeh [a], Okan Sirin [a,*,1], Mohammed Sadeq [b], Haissam Sebaaly [c], Eyad Masad [d]

[a] Department of Civil and Architectural Engineering, Qatar University, P.O.Box 2713, Doha, Qatar
[b] Seero Engineering Consulting, P.O.Box 201257, Doha, Qatar
[c] Department of Civil Engineering, University of Pretoria, Private Bag X20 Hartfield, 0028 Pretoria, South Africa
[d] Mechanical Engineering Program, Texas A&M University at Qatar, P.O.Box 23874, Doha, Qatar

ARTICLE INFO

Keywords:
Hirsch model
Alkhateeb model
Dynamic modulus
Mechanistic-Empirical Pavement Design
Qatar

ABSTRACT

The dynamic modulus ($|E^*|$) of asphalt mixtures is one of the most important inputs in Mechanistic-Empirical (ME) pavement analysis and design. Several models have been developed to predict the dynamic modulus based on mixture volumetrics and material properties. This study aimed to calibrate and validate two commonly used models (i.e., Hirsch model and Alkhateeb model) for predicting the dynamic modulus of asphalt mixtures in Qatar. Based on the study outcomes, the Hirsch model was found to have a high prediction performance of asphalt mixture moduli before calibration with a coefficient of determination (R^2) of 87.2 % between predicted and measured values. This R^2 value improved slightly after calibration to 89.2 %, Alkhateeb model, on the other hand, had a coefficient of determination of 70.8 % before calibration, which also improved to 89.2 % after calibration. The moduli predicted by the Hirsch model before and after calibration were employed in this study to perform a mechanistic-empirical analysis of the performance of various typical pavement sections in Qatar. According to the findings, the percentage change in the predicted fatigue damage due to the use of the calibrated Hirsch model reached more than 50 % with an average value of 17.33 %, while the percent change in rutting reached 14 % with an average value of 3.65 %. These results highlight the importance of using locally calibrated models for the dynamic modulus in order to improve performance predictions.

1. Introduction

Dynamic modulus ($|E^*|$) of asphalt mixtures is an important parameter in pavement design as it is used as the main input for the Mechanistic-Empirical (ME) pavement design method. Furthermore, the dynamic modulus is used to determine the layer coefficients of asphalt layers in the AASHTO 1993 empirical design method [1,2]. However, the cost and time duration required for experimentally determining the dynamic moduli have been a barrier for its use by pavement designers and researchers. In addition, materials may not be readily available during the pavement design stage to prepare mixtures and experimentally measure their dynamic moduli. As a

* Corresponding author.
E-mail addresses: aa2000369@student.qu.edu.qa (A. Al-Tawalbeh), okansirin@qu.edu.qa (O. Sirin), mohammed.sadeq@seeroeng.com (M. Sadeq), u17404054@tuks.co.za (H. Sebaaly), eyad.masad@qatar.tamu.edu (E. Masad).
[1] ORCID: 0000-0002-5124-1061.

https://doi.org/10.1016/j.cscm.2022.e01580
Received 16 May 2022; Received in revised form 6 August 2022; Accepted 14 October 2022
Available online 17 October 2022

result, several studies have concentrated on constructing predictive equations that estimate the dynamic modulus based on the volumetrics of the mix and the properties of its components (e.g., asphalt binder and aggregate) [3–7]. Various models have been developed and evaluated, each with its own set of assumptions, prediction approaches, and accuracy. Several dynamic modulus prediction models (e.g., Hirsch Model, Alkhateeb Model, Witzack 1-37A, and Witzack 1-40D) have been widely used in practice [8]. Hirsch and Alkhateeb models were developed based on the interactive physical behavior between asphalt binder and aggregate with regression and statistical fitting. They have more straightforward formulations and require fewer inputs than the Witzack 1-37A and Witzack 1-40D models, which are entirely based on multivariate regression analysis [9].

Hirsch model was utilized to determine the sensitivity of the dynamic modulus to volumetrics [10]. Christensen et al. [3] compared various Hirsch model versions and recommended a specific formulation that is the most used today. It is a semi-empirical model that is developed based on mechanics concepts of composite materials and regression results [11]. However, the Hirsch model's empirical part, based on a conventional mixtures' dataset, requires further calibration using local sets of measurements to enhance the accuracy of the model.

Alkhateeb model assumes that asphalt mixture's performance is a combination of series and parallel composite models. The dataset used in the original model development includes modified and unmodified asphalt mixtures with a wide range of binder performance grades [4]. Two follow-up studies revealed that Alkhateeb model produced biased predictions at low temperatures [12,13].

Several researchers evaluated Hirsch and Alkhateeb models using the results of testing local asphalt mixtures [8,14,15]. Yousefdoost et al. [12] evaluated Hirsch, Alkhateeb, Witzack 1-37A, and Witzack 1-40D dynamic modulus prediction models for Australian asphalt mixtures. The study concluded that both the Alkhateeb and Hirsch models underpredict the dynamic moduli of Australian asphalt mixtures. Robbins and Timm [8] conducted a study to evaluate Witzack 1-37A, Witzack 1-40D, and Hirsch models for South-eastern United States asphalt mixtures and concluded that the Hirsch model underpredicts the dynamic modulus at 4.4 °C (40 °F) and 37.8 °C (100 °F) and over-predicts at 21.1 °C (70 °F).

Far et al. [13] studied the Alkhateeb, Hirsch, Witzack 1-37A, and Witzack 1-40D models and developed an Artificial Neural Network (ANN) dynamic modulus prediction model. According to the study, in comparison to the 1-40D Witzack and Hirsch models, the Alkhateeb model showed a considerable bias at low temperatures. Furthermore, both the modified Witzack and Hirsch models exhibited substantial bias at high temperatures, as well as insensitivity to volumetric parameters.

Solatifar [15] compared the performance of six dynamic modulus prediction models (Hirsch, Witzack 1-37A, Witzack 1-40D, Alkhateeb, Global, and Simplified Global). The study used a published database of 1320 dynamic modulus test points of 66 asphalt mixtures evaluated by the University of Maryland at a wide range of frequencies and temperatures. The main outcome was a descending order of the six investigated models based on prediction performance, where Hirsch and Alkhateeb models came as fourth and fifth, respectively. The conclusion was that all models could be used to determine the dynamic modulus with proper calibrations using local materials and mixtures.

Several studies calibrated the Hirsch and Alkhateeb models to improve the prediction performance. Robbins and Timm [8] replaced the regression constant of 4,200,000 with the local aggregate Young's modulus and used error minimization to find new fitting factor values. The research demonstrated a slight improvement of 1.4 % in R^2 for Hirsch model prediction and concluded that local calibration is not required in this case. Shen et al. [16] calibrated the Hirsch model to better fit a number of asphalt mixtures by replacing the regression constant of 4,200,000 with 4,800,000. In addition, the research defined new regression constants (0.2, 600, and 0.56) instead of the values (20, 650, and 0.58) used in the original model. This calibration improved the overall prediction performance of the Hirsch model; however, the modified version overpredicted the dynamic modulus at high testing temperatures.

Khattab et al. [17] evaluated Witzack 1-37A and 1-40D dynamic modulus prediction models to study the implementation of AASHTOWare-Pavement ME Design in Saudi Arabia. This study involved 25 different HMA mixtures, and the results showed that the performance of the two models is sensitive to temperature and the binder type. The study concluded that both models have biased predictions at low temperatures. At high testing temperatures, both models had a lower bias.

El-Badawy et al. [18] applied the Artificial Neural Network (ANN) technique for E* prediction based on 25 asphalt mixtures and considered the inputs of Witzack 1-37A, Witzack 1-40D, and Hirsch models. After determining the most sensitive inputs using global sensitivity analysis (GSA) and commercially available software, ANN models were found to be more accurate than conventional models. The study concluded that the Hirsch model lacks parameters representing the aggregate characteristics, negatively affecting the model accuracy.

Moussa and Owais [5] developed a Deep Convolution Neural Networks (DCNNs) technique based on six convolution blocks and applied it to Witzack 1-37A and Witzack 1-40D. The study concluded that the developed models based on machine learning have a higher performance than conventional prediction models. In another research [6], a prediction model-based Deep Residual Neural Networks (DRNNs) technique was developed based on comparing 8191 combinations of inputs. The results showed that the DRNNs model outperformed the conventional E* prediction models (Witczak 1-37A, Witczak 1-40D, and Hirsch).

Cooper et al. [19] conducted a study to evaluate the effect of dynamic modulus values on pavement performance predictions. For this purpose, ten mixtures were sampled during the design, production, and construction stages. Consequently, Mechanistic-Empirical (ME) pavement analysis was conducted using AASHTOWare. The analysis showed that rutting distresses were sensitive to the dynamic modulus. Moreover, it was found that the difference in the predicted alligator cracking between plant-produced laboratory-compacted (PL) specimens and field cores of the same mixture reached 60 % due to the change in the dynamic modulus. Cheng et al. [20] conducted a study to evaluate the effect of the loading mode on the dynamic modulus value and, consequently, on the predicted pavement performance. The study considered three loading modes: uniaxial compression (UC), indirect tension (IDT), and four-point bending (4PB). It was found that field strain responses vary significantly when using different types of dynamic modulus in the MEPDG procedure.

Qatar has witnessed exponential growth in all infrastructure sectors and wide expansion in road networks for the past two decades. During this development, the need to provide value-engineered and sustainable pavement structures has become a priority. Qatar Highway Design Manual (QHDM) [21] and Interim Advice Note No. 101 [22] of the Public Works Authority (PWA) of Qatar have recommended using the Hirsch model to predict the dynamic modulus of asphalt layers. Since the Hirsch model was developed based on the USA mixtures [3], the prediction performance of the Hirsch model of Qatar-based mixtures required further verification and possibly recalibration of the model.

This paper aims to validate and calibrate Hirsch and Alkhateeb models using Qatar's local materials and climate. Additionally, this study assesses the sensitivity of the calibrated models' to material properties, temperature, and frequency. This is followed by studying the effect of calibration on the fatigue and rutting performance of Qatar's typical pavement structures.

2. Models description

2.1. Hirsch model

The development of the Hirsch model considers the binder and aggregate to be connected through a combined series and parallel models, as shown in Eq. (1) [7].

$$|E^*|_m = x(E_1V_1 + E_2V_2) + (1-x)\left(\frac{V_1}{E_1} + \frac{V_2}{E_2}\right)^{-1} \tag{1}$$

Where:

$|E^*|_m$ = Predicted asphalt mixture dynamic modulus
x = Percent of series behavior in the mixture
E_1 = Aggregate modulus
V_1 = Aggregate volume
E_2 = Binder modulus
V_2 = Binder volume

Eqs. (2)–(4) represent the version of the Hirsch model that considers a mixture of volumetric components and binder properties [3,7].

$$|E^*|_m = Pc\left[4,200,000\left(1-\frac{VMA}{100}\right) + 3|G^*|_b\left(\frac{VFA * VMA}{10,000}\right)\right] + (1-Pc)\left[\frac{1-\frac{VMA}{100}}{4,200,000} + \frac{VMA}{3VFA\ |G^*|_b}\right]^{-1} \tag{2}$$

Where:

$$Pc = \frac{(20+a)^{0.58}}{650+(a)^{0.58}} \tag{3}$$

where:

VMA = Voids in the mineral aggregate (%)
VFA = Fraction of aggregate voids filled with asphalt (%)
$|G^*|_b$ = Dynamic modulus of the binder (asphalt) (psi)

$$a = \frac{VFA * 3|G^*|_b}{VMA} \tag{4}$$

The constants (20, 0.58, and 650) are fitting parameters obtained from regression analysis and fitting with measured moduli of asphalt mixtures [10]. The constant (4,200,000) is an assumed aggregate young's modulus (in psi). The constant (3) multiplied with the $|G^*|_b$ is obtained by assuming that asphalt is an incompressible material with a Poisson's ratio (ν) of 0.5 substituted in the elastic modulus (E) equation: $E = 2(1+\nu)|G^*|_b$, where ($|G^*|_b$) is the binder modulus [10].

2.2. Alkhateeb model

Alkhateeb model [4] has also been used in pavement analysis and design as it requires a small number of inputs to predict the dynamic modulus $|E^*|$ or $|G^*|$. This model was developed based on the law of mixtures considering the three-phase system of aggregate, binder, and air voids. Alkhateeb determined the fitting parameters using mixtures from the State of Virginia in the USA. The set of

mixtures included the aged and modified binders. Eq. (5) represents the Alkhateeb model [4].

$$|E^*|_m = 3 \quad \left(\frac{100 - VMA}{100}\right)\left(\frac{\left(90 + 1.45\left(\frac{|G^*|_b}{VMA}\right)^{0.66}\right)}{1100 + \left(0.13\left(\frac{|G^*|_b}{VMA}\right)^{0.66}\right)}\right)|G^*|_g \tag{5}$$

Where:

VMA = Voids in the mineral aggregate (%)
VFA = Fraction of aggregate voids filled with asphalt (%)
$|G^*|_b$ = Complex modulus of the binder (asphalt) (psi)
$|G^*|_g$ = Dynamic shear modulus of binder in the glassy state in Pa (assumed to be 10^9 Pa)

2.3. Models comparison

Table 1 shows the main inputs for Hirsch and Alkhateeb model based on the reviewed literature. Al-Khateeb et al. [4] stated their dataset contains a wide range of both modified and unmodified materials relative to the dataset used for calibrating the Hirsch model.

3. Qatar climate conditions

The climate condition is an essential input in determining the properties of pavement materials. Qatar has a hot desert climate with high humidity levels during the summer. According to the Qatar Meteorology Department, Doha has a low average annual rainfall precipitation of 79 mm [24]. Fig. 1 shows the climatic temperature in Qatar for the period 1962–2013 collected in Doha city station [25].

There is no significant deviation in the overall terrain and environment of the State of Qatar; thus, the data collected from Doha station represents the entire country's climate. Fig. 1 shows that the lowest temperature throughout the year is 13.5 ℃. This explains that the State of Qatar does not experience air temperatures of 4 or 5 ℃, which are typically used in dynamic modulus testing to construct the master curve.

4. Binder and mixture master curves

The master curve equation of the binder dynamic modulus and mixture dynamic modulus considered in this study is represented in Eq. (6) [26].

$$\log \quad |M^*| = \delta + \frac{\alpha}{1 + e \quad ^{-\beta} \quad - \quad \gamma.\log \quad f_r} \tag{6}$$

Where $|M^*|$ is the modulus value of either the mixture $|E^*|$ or binder $|G^*|$; (δ, α, β, and γ) are the fitting parameters; and f_r is the reduced frequency defined in Eq. (7) [26].

$$f_r = f.a(T) \tag{7}$$

Where $a(T)$ is the temperature shift factor coefficient that can be calculated using Eq. (8) [26].

$$\log(a(T)) = a_1\left(T^2 - \quad T_{ref}^2\right) + a_2\left(T - T_{ref}\right) \tag{8}$$

Where (a_1 *and* a_2) are the temperature shift factors and (T *and* T_{ref}) are the actual temperature and reference temperature, respectively.

Binder master curve parameters are collected from two studies conducted in Qatar [27,28] in order to find the $|G^*|_b$ that needed to

Table 1
Main inputs for the Hirsch and Alkhateeb models.

Criterion	Hirsch model	Alkhateeb model
Prediction type	Semi-empirical [10]	Semi-empirical [4]
Number of Test points	206 [3]	150 [4]
Number of Mixes	18 [3]	6 [4]
Type of Binders	2 Unmodified and 2 Modified [3]	6 Types of Modified and Unmodified [4,12]
Aggregate Gradation	1 Dense, 3 Fine, and 1 Coarse [3]	1 Dense [4,12]
Aging	Short-term Aged [23]	Short-term Aged [4,12]
Testing Waves	Haversine [23]	Haversine [4]
Assumed Mechanical Response	Two Phases in parallel and series [3]	Three phases in parallel [4]

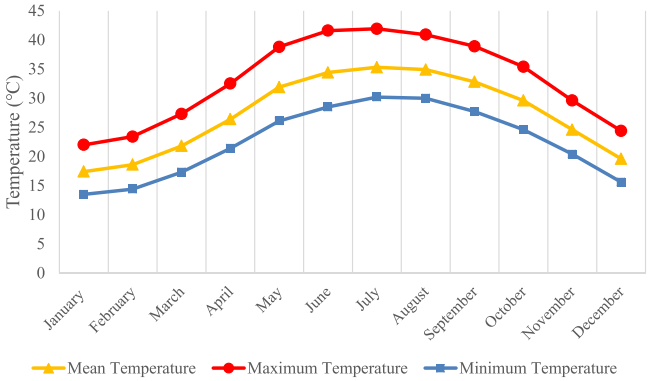

Fig. 1. Climatic temperature normals in Qatar for the period 1962–2013 (Qatar Meteorology Department: Doha Station).

predict the binder dynamic moduli in both Hirsch and Alkhateeb models at different frequencies and temperatures. The collected binder types represent the country's most common binders used in recently constructed road projects. The dataset includes unmodified binder, Polymer Modified Binder (PMB) containing styrene-butadiene-styrene (SBS), Crumb Rubber Modified Binder (CRMB), and Reclaimed Asphalt Binder (RAB) with different mixing percentages mixed with unmodified PEN 60/70 (PG64S-22) binder. All materials are approved for use in Qatar depending on the type of pavement structure and loading level. The dataset represents a wide range of Superpave PG grading. The binder types and relevant master curve coefficients are presented in Table 2.

Twenty asphalt mixtures master curves are collected from several research studies [27–29] and construction projects in Qatar. The collected data set included mixtures used in the Wearing Course (WC) and Asphalt Base Course (ABC) with 19 and 25 mm Nominal Maximum Aggregate Size (NMAS), respectively. The asphalt mixtures represented the materials and designs used in the country and were tested based on Qatar Construction Specification (QCS 2014) [30]. The binder content percentage (BC%) of the collected data ranges between 3.4 % and 4.3 %, while the Air Void ratio (V_a) of the test specimens ranges between 5.2 % and 7.0 %. The master curve coefficients of the collected mixtures are presented in Table 3. The composition and volumetrics of these collected mixtures are shown in Table 4.

5. Model calibration

For the validation and calibration of the Hirsch and Alkhateeb models, 393 measured dynamic moduli for 20 mixtures are used for comparison with the predicted values from the two models. As shown in Table 5, a wide range of frequencies and temperatures are represented in the collected dataset.

After comparing the Hirsch and Alkhateeb models' predicted dynamic modulus values versus the measured ones, the coefficient of determination (R^2) and S_e/S_y values were computed as goodness-of-fit measures using Eqs. (9)–(11) [12].

$$R^2 = 1 - \frac{(n-k-1)}{(n-1)}\left(\frac{S_e}{S_y}\right)^2 \tag{9}$$

Where:

n = Number of testing points
k = Number of regression coefficients in the prediction model
S_e = Standard error of estimation
S_y = Standard deviation of the measured values

Table 2
Binder types and coefficients of binder master curves.

Binder type	Binder grade	Master curve coefficients						
		δ	α	β	ɣ	a_1	a_2	T_{ref} (°C)
Unmodified	PEN 60/70[a]	-0.7380	8.8480	-0.0330	0.5880	0.0010	-0.1690	46.0
PMB	PG 76E-10	-0.9450	10.4730	0.0960	0.3080	0.0007	-0.1430	46.0
CRMB	PG 76E-10	1.5470	7.3020	0.5445	0.3925	0.0008	-0.1511	21.0
15 % RAB	PG 70S-22	0.0000	8.4598	0.0954	0.4221	0.0007	-0.1438	46.0
25 % RAB	PG 70S-22	0.0514	8.3672	0.2467	0.4401	0.0007	-0.1438	46.0
35 % RAB	PG 70S-22	0.7145	7.9034	0.0001	0.4414	0.0007	-0.1437	46.0

[a] PEN 60/70 binder is equivalent to grade PG64-22.

Table 3
Coefficients of mixture master curves.

HMA no.	Master curve coefficients						
	δ	α	β	γ	a_1	a_2	T_{ref} (°C)
1	1.3309	3.1640	1.1334	0.3973	0.000610	-0.164685	20
2	1.8844	2.4852	1.0388	0.5557	0.000720	-0.164155	20
3	1.2225	3.1417	1.2301	0.5229	0.001994	-0.216857	20
4	-7.9430	12.8600	2.3860	0.1690	0.000831	-0.178000	21
5	-2.1850	6.9960	1.6330	0.2560	0.000737	-0.172243	20
6	-2.3190	6.9330	1.8690	0.2780	0.000899	-0.180347	20
7	-2.2800	6.8980	1.7860	0.2660	0.000948	-0.174775	20
8	-2.2210	6.8700	1.7580	0.2660	0.001050	-0.184469	20
9	-2.2280	6.7510	2.0530	0.2750	0.000920	-0.176847	20
10	-2.4620	7.0660	1.8630	0.2810	0.001206	-0.192653	20
11	-2.2700	6.9550	1.8850	0.2370	0.000952	-0.176755	20
12	-2.1560	6.8590	2.0260	0.2650	0.001154	-0.191043	20
13	-0.3760	4.9740	1.5660	0.2910	0.000510	-0.151924	20
14	-2.1410	6.7370	1.7590	0.2730	0.000720	-0.161181	20
15	-2.3330	6.8840	2.0900	0.3700	0.001066	-0.178346	20
16	-2.2560	6.8740	2.1550	0.2720	0.000691	-0.169981	20
17	4.3980	-1.8998	-0.1937	-0.5781	0.000376	-0.137171	20
18	4.3755	-2.0522	-0.6525	-0.5910	0.000664	-0.150427	20
19	4.4333	-2.2062	-0.6040	-0.4591	0.000118	-0.124096	20
20	4.4018	-1.9586	-0.7128	-0.4767	0.000263	-0.134852	20

Table 4
Mixtures composition and volumetrics at test conditions.

HMA no.	Binder type	Binder grade	Mixture rule	NMAS [mm]	Aggregate type	BC%	V_a [%]	VMA [%]	VFA [%]
1	PMB	PG76E-10	ABC	25	Gabbro	4.10	6.10	16.20	62.60
2	PMB	PG76E-10	WC	19	Gabbro	4.30	6.00	15.80	61.90
3	Unmodified	PEN60/70	ABC	25	Gabbro	3.40	6.65	15.00	55.70
4	CRMB	PG76E-10	ABC	25	Gabbro	3.90	6.70	16.10	58.40
5	Unmodified	PEN60/70	WC	19	Gabbro	3.90	6.20	15.80	60.80
6	Unmodified	PEN60/70	WC	19	Gabbro	3.80	6.50	15.90	59.10
7	Unmodified	PEN60/70	WC	19	Gabbro	3.40	6.40	14.70	56.50
8	Unmodified	PEN60/70	WC	19	Gabbro	3.60	6.50	15.50	58.10
9	Unmodified	PEN60/70	WC	19	Gabbro	3.90	6.70	16.50	59.40
10	Unmodified	PEN60/70	WC	19	Gabbro	4.10	5.20	14.60	64.40
11	PMB	PG76E-10	WC	19	Gabbro	4.30	6.10	15.30	60.10
12	PMB	PG76E-10	WC	19	Gabbro	4.10	6.00	14.40	58.30
13	PMB	PG76E-10	WC	19	Gabbro	4.10	5.20	14.20	63.40
14	PMB	PG76E-10	WC	19	Gabbro	4.00	5.90	14.80	60.10
15	PMB	PG76E-10	WC	19	Gabbro	4.30	6.00	15.70	61.80
16	PMB	PG76E-10	WC	19	Gabbro	4.30	5.70	15.00	62.00
17	Unmodified	PEN60/70	ABC	25	Gabbro	3.90	6.90	14.70	53.20
18	15 % RAB	PG70S-22	ABC	25	Gabbro	3.70	6.80	14.70	53.40
19	25 % RAB	PG70S-16	ABC	25	Gabbro	3.50	6.90	14.70	53.10
20	35 % RAB	PG76S-10	ABC	25	Gabbro	3.50	6.90	15.40	55.20

Table 5
Testing temperatures and frequencies of mixtures dataset.

Group no.	HMA no.[a]	Temperature (℃)	Frequency (Hz)
Group 1	1, 2, 3, 4	4, 20, and 45	0.1, 1.0, and 10
Group 2	5, 6, 7, 8, 9, 10	4, 40, and 40	0.1, 0.2, 0.5, 1.0, 2.0, 5.0, 10.0, and 20.0
Group 3	11, 12, 13, 14, 15, 16	4, 20, and 45	0.1, 0.2, 0.5, 1.0, 2.0, 5.0, 10.0, and 20.0
Group 4	17, 18, 19, 20	5, 15, 25, 35, 45	0.1, 1.0, and 10.0

[a] HMA numbers based on Tables 3 and 4.

where:

$$S_y = \sqrt{\frac{\sum_{i=1}^{n}(E^*_{mi} - \overline{E}^*_m)^2}{(n - 1)}} \quad (10)$$

$$S_e = \sqrt{\frac{\sum_{i=1}^{n}(E^*_{pi} - \overline{E}^*_{mi})^2}{(n - k - 1)}} \quad (11)$$

where:

E^*_{mi} = Measured dynamic modulus value
$\overline{E}^*_m$ = Average of dynamic modulus measured values
E^*_{pi} = Dynamic modulus predicted value

In order to interpret the computed values of R^2 and S_e/S_y, the criteria in Table 6 are followed [31].

Statistical bias has also been used to determine both models' predictive performance by finding the slope and intercept of the linear trend line of the measured vs. predicted plot. The higher prediction performance would be subjected to a slope closer to One and an intercept closer to Zero [15].

To calibrate the models, the Excel solver is utilized to minimize the error and maximize the fit (i.e., R^2 value). The error is computed using Route Mean Square Error (RMSE) formula in Eq. (12) [32].

$$RMSE = \sqrt{\frac{\sum_{i=1}^{n}(E^*_{mi} - E^*_{pi})^2}{n}} \quad (12)$$

Where:

RMSE = Route Mean Square Error

Based on the error minimization results, new fitting parameters for the Hirsch model (i.e., h_1–h_3) are determined instead of 20, 650, and 0.58, respectively, in Eq. (2). The same approach is followed for the Alkhateeb model to find k_1–k_6 coefficients instead of 3, 90, 1.45, 0.66, 1100, and 0.13, respectively, in Eq. (5).

6. Results and discussion

The R^2 value of prediction performance for the Hirsch model before and after calibration is 87.2 % and 89.2 %, respectively. Figs. 2 and 3 show measured versus predicted E* before and after calibration of the Hirsch model, respectively. The R^2 value of prediction performance for the Alkhateeb model before and after calibration is 70.8 % and 89.2 %, respectively. Figs. 4 and 5 show measured versus predicted E* before and after calibration of the Alkhateeb model, respectively.

Table 7 shows the goodness-of-fit measures and their correlation for both Hirsch and Alkhateeb models before and after calibration.

Table 8 shows bias measures for both Hirsch and Alkhateeb models before and after calibration.

As presented in Tables 7 and 8, the Hirsch model shows high prediction performance without calibration with an R^2 value of 87.2 %. After calibration, the R^2 value improved slightly to 89.2 %. This improvement of 2 % in R^2 value matches the study of Robbins and Timm [8] for the southeastern United States asphalt mixtures that used a similar error minimization approach to improve the Hirsch model R^2 value from 89.7 % to 91.1 %.

Alkhateeb model shows reasonable prediction performance prior to calibration over a wide range of frequencies and temperatures. However, the model underpredicts the dynamic modulus (E*) values at a significant number of testing points with exponential trends resulting in a low R^2 value of 70.8 %. The calibration of the model improved the R^2 value to become 89.2 %. The predictive performance of both the Hirsch and Alkhateeb models comes contrary to Yousefdoost et al. [12] study, which concluded that the Hirsch

Table 6
Statistical criteria for correlation between measured and predicted E*.

Criteria	R^2 (%)	S_e/S_y
Excellent	> 90	< 0.35
Good	70–89	0.36–0.55
Fair	40–69	0.56–0.75
Poor	20–39	0.76–0.90
Very Poor	< 19	> 0.90

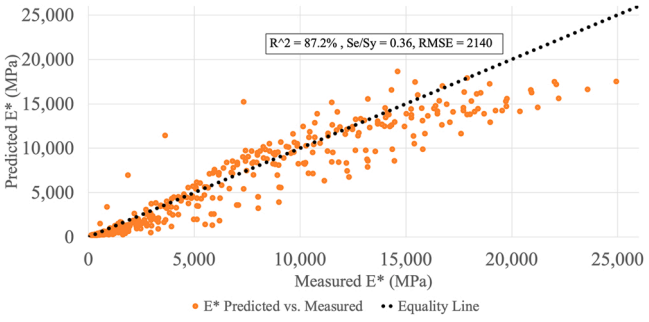

Fig. 2. Predicted vs. measured E* before calibration – Hirsch model.

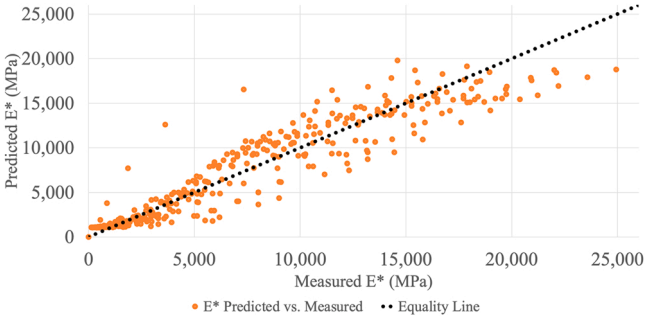

Fig. 3. Predicted vs. measured E* after calibration – Hirsch model.

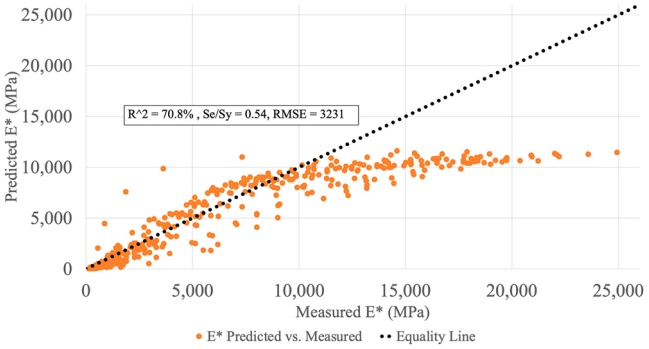

Fig. 4. Predicted vs. measured E* before calibration – Alkhateeb model.

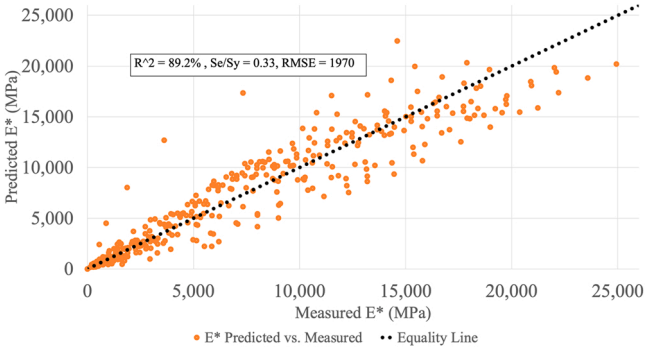

Fig. 5. Predicted vs. measured E* after calibration – Alkhateeb model.

Table 7
Hirsch and Alkhateeb overall models goodness-of-fit values.

Model	Before calibration				After calibration			
	R^2 (%)	Correlation	Se/Sy	Correlation	R^2 (%)	Correlation	Se/Sy	Correlation
Hirsch	87.2	Good	0.36	Good	89.2	Good	0.33	Excellent
Alkhateeb	70.8	Good	0.54	Good	89.2	Good	0.33	Excellent

Table 8
Hirsch and Alkhateeb overall models bias measures.

Model	Before calibration		After calibration	
	Slope	Intercept	Slope	Intercept
Hirsch	0.848	214.370	0.900	716.980
Alkhateeb	0.612	1116.100	0.900	652.750

and Alkhateeb models do not fit well for Australian asphalt mixtures.

Sensitivity analysis was conducted for the calibrated Hirsch and Alkhateeb models to investigate the sources of prediction errors and relate the results to the local Qatar conditions. R^2 and S_e/S_y were calculated for the prediction performance for both Hirsch and Alkhateeb models by varying one factor of binder type, temperature, or frequency at a time while keeping the other factors constants. Tables 9 and 10 present the R^2 values of the Hirsch and Alkhateeb models for several binder types, respectively. Tables 11 and 12 show the R^2 of the Hirsch and Alkhateeb models, respectively, for several testing temperatures.

Tables 13 and 14 present the R^2 of the calibrated Hirsch and Alkhateeb models for several frequencies' values, respectively.

Based on the sensitivity analysis results, it can be concluded that the calibrated Alkhateeb model shows equivalent performance to the calibrated Hirsch model for all types of binder mixtures. However, uncalibrated models offer the good superior performance of the Hirsch model in a PEN60/70 and PG 76E-10 but lower performance in RAB mixtures. This can be because the Alkhateeb model was developed using a dataset of aged materials [4]. It is noticed that the calibration reduced the prediction performance of both models for RAB mixtures.

For testing frequency sensitivity, the uncalibrated Hirsch model shows superior performance over the Alkhateeb model, which has a significantly increasing bias toward higher frequencies. After calibration, the Alkhateeb model bias at high frequency is reduced significantly.

For temperature sensitivity, both uncalibrated models show poor predictive performance at high test temperatures of 35–45 ℃, which improved after calibration. This finding agrees with Far et al. [13], who showed a noticeable bias of the Hirsch model at high test temperatures. By examining Fig. 4, Tables 12, and 14, it can be concluded that the uncalibrated Alkhateeb model has a poor prediction performance at test temperatures 4–5 ℃ and 10–20 Hz frequencies, which improved after calibration (Fig. 5). This result agrees with the studies of Yousefdoost et al. [12] and Far et al. [13]. The Hirsch model's performance at low temperatures was better than the Alkhateeb model, which agrees with Far et al. [13]. However, the low predictability at such low temperatures is not a concern in Qatar because these temperatures are rare, as shown in Fig. 1. Tables 15 and 16 show the fitting parameters for Hirsch and Alkhateeb models, respectively.

7. Pavement performance analysis

This section compares the performance of pavement structures typically used in Qatar, considering the dynamic modulus of the Hirsch Model before and after calibration. This was accomplished by evaluating the rutting and fatigue cracking performance using the Mechanistic-Empirical Asphalt Pavement Analysis (MEAPA) web application developed by Kutay and Lanotte [33]. This web-based application considers the same traffic inputs of the NCHRP 1-37A Mechanistic-Empirical Pavement Design Guide (MEPDG) [34]. The climatic model in MEAPA is very similar to the Enhanced Integrated Climatic Model (EICM) in the MEPDG. Eq. (6) presented earlier in this paper is considered in the MEAPA application to represent the master curve. The calculation of the loading frequency is based on the concepts used by the MEPDG, where the stress pulse is assumed to be haversine, and its duration depends upon the vehicle speed and the depth of the point of interest below the pavement surface. The Global Aging System (GAS) model is considered to define the effect of aging (due to heat and oxidation) on the modulus of the AC sublayers. In addition, the basic propagation of the thermal crack length within the depth of the pavement is found based on a simplified Paris law. MEAPA application has several climatological profiles covering several areas and climates worldwide that can be chosen as preliminary analysis to have a more accurate site-specific simulation.

Three pavement structures for different road hierarchies and traffic loading conditions are employed in the analysis to simulate the actual pavement structures used in Qatar. Fig. 6 shows pavement structures for the collected three pavement sections for different road reliabilities of 75 %, 90 %, and 97 % corresponding to local, arterial, and expressway road hierarchies, respectively, based on Qatar Highway Design Manual (QHDM) [21]. The selected three pavement structures have three different traffic loading levels expressed as the number of design Equivalent Single Axle Loads (ESALs). Fig. 7 shows a binder-type matrix for the collected pavement structures for the asphalt Wearing Course (WC), Asphalt Intermediate Course (AIC), and Asphalt Base Course (ABC) layers.

Table 9
Binder sensitive predictive performance of the calibrated Hirsch model.

Binder type			PEN 60/70		PG 76E-10		RAB (15, 25, 35) %	
No. of data points			169		164		45	
Calibration	**Before**	**R^2**	94.40 %	Excellent	86.40 %	Good	63.10 %	Fair
		Se/Sy	0.24	Excellent	0.37	Good	0.63	Fair
	After	**R^2**	94.60 %	Excellent	90.50 %	Excellent	50.90 %	Fair
		Se/Sy	0.23	Excellent	0.31	Excellent	0.73	Fair

Table 10
Binder sensitive predictive performance of the calibrated Alkhateeb model.

Binder type			PEN 60/70		PG 76E-10		RAB (15, 25, 35) %	
No. of data points			169		164		45	
Calibration	**Before**	**R^2**	78.6 %	Good	65.9 %	Fair	70.8 %	Good
		Se/Sy	0.47	Good	0.59	Fair	0.58	Fair
	After	**R^2**	95.1 %	Excellent	91.1 %	Excellent	41.2 %	Fair
		Se/Sy	0.23	Excellent	0.30	Excellent	0.83	Poor

Table 11
Temperature sensitive predictive performance of the calibrated Hirsch model.

Temperature			4 and 5 ℃		15, 20 and 25 ℃		35, 40, and 45 ℃	
No. of data points			122		134		137	
Calibration	**Before**	**R^2**	35.6 %	Poor	42.8 %	Fair	17.5 %	Very Poor
		Se/Sy	0.81	Poor	0.77	Poor	0.92	Very Poor
	After	**R^2**	51.0 %	Fair	40.6 %	Fair	36.9 %	Poor
		Se/Sy	0.71	Fair	0.78	Poor	0.80	Poor

Table 12
Temperature sensitive predictive performance of the calibrated Alkhateeb model.

Temperature			4 and 5 ℃		15, 20 and 25 ℃		35, 40 and 45 ℃	
No. of data points			122		134		137	
Calibration	**Before**	**R^2**	-94.8 %	Very Poor	53.9 %	Fair	15.0 %	Very Poor
		Se/Sy	1.41	Very Poor	0.69	Fair	0.93	Very Poor
	After	**R^2**	48.6 %	Fair	44.4 %	Fair	38.4 %	Poor
		Se/Sy	0.73	Fair	0.75	Fair	0.79	Poor

Table 13
Frequency sensitive predictive performance of the calibrated Hirsch model.

Frequency (Hz)	n[a]	Before calibration				After calibration			
		R^2		Se/Sy		R^2		Se/Sy	
0.1	68	78.30 %	Good	0.48	Good	81.90 %	Good	0.44	Good
0.2	39	81.70 %	Good	0.45	Good	84.90 %	Good	0.40	Good
0.5	36	88.50 %	Good	0.36	Good	90.70 %	Excellent	0.32	Excellent
1	68	89.00 %	Good	0.34	Excellent	89.90 %	Good	0.32	Excellent
2	36	90.00 %	Excellent	0.33	Excellent	92.80 %	Excellent	0.28	Excellent
5	36	89.40 %	Good	0.34	Excellent	92.50 %	Excellent	0.29	Excellent
10	68	83.40 %	Good	0.42	Good	83.70 %	Good	0.41	Good
20	39	84.60 %	Good	0.41	Good	88.90 %	Good	0.35	Excellent

[a] n = Number of data points.

In the MEAPA web application, the nearest available climatological profile to the State of Qatar was for Dammam city, located in the eastern area of Saudi Arabia. Dammam city is 180 km air distance from Doha city, the capital of the State of Qatar. In order to validate the use of Dammam city climatological profile to represent Qatar, monthly mean temperatures data for Dammam was collected from the Saudi National Center for Meteorology (NCM) website [35] and compared with the data collected from the Qatar Meteorology Department website [25]. Fig. 8 shows the mean monthly temperature normals for Doha and Dammam cities. As shown in

Table 14
Frequency sensitive predictive performance of the calibrated Alkhateeb model.

Frequency (Hz)	n[a]	Before calibration				After calibration			
		R^2		Se/Sy		R^2		Se/Sy	
0.1	68	80.60 %	Good	0.46	Good	83.80 %	Good	0.42	Good
0.2	39	80.40 %	Good	0.48	Good	86.50 %	Good	0.40	Good
0.5	36	80.60 %	Good	0.48	Good	91.20 %	Excellent	0.33	Excellent
1	68	78.70 %	Good	0.48	Good	89.00 %	Good	0.35	Excellent
2	36	71.50 %	Good	0.59	Fair	92.60 %	Excellent	0.30	Excellent
5	36	63.70 %	Fair	0.66	Fair	92.60 %	Excellent	0.30	Excellent
10	68	59.70 %	Fair	0.67	Fair	81.70 %	Good	0.45	Good
20	39	47.30 %	Fair	0.79	Poor	90.20 %	Excellent	0.34	Excellent

[a] n = Number of data points.

Table 15
Fitting parameters for the Hirsch model (Eq. (2)).

Fitting factor	Before calibration	After calibration
h_1	20	348
h_2	650	897
h_3	0.58	0.63

Table 16
Fitting parameters for the Alkhateeb model (Eq. (5)).

Fitting factor	**Before calibration**	**After calibration**
k_1	3.00	6.76
k_2	90.00	92.69
k_3	1.45	2.67
k_4	0.66	0.42
k_5	1100.00	255.69
k6	0.13	0.01

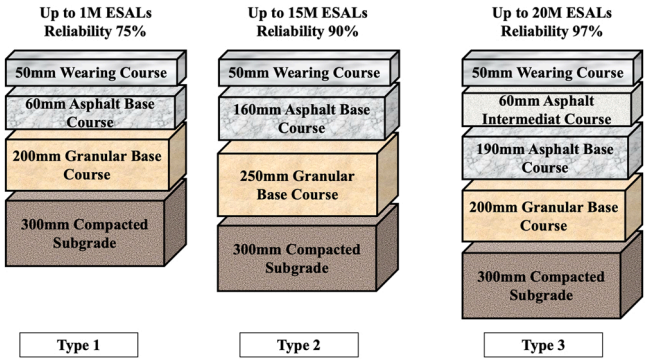

Fig. 6. Illustration of three pavement structures.

Fig. 8, Doha and Dammam have similar mean temperature climatological normals with only minor differences. Accordingly, Dammam's climatological profile is considered valid to represent Qatar climate. Table 17 shows the traffic inputs used in the ME analysis on the MEAPA website.

It is to be noted that vehicle class distribution, monthly distribution, and axle load distribution were kept as default in the MEAPA software. Table 18 shows the performance results and percent change before and after calibration for pavement structures Type 1, 2, and 3.

As shown in Table 18, the difference in the predicted distress, whether a decrease or increase due to calibration, is more significant in the fatigue life predictions than the rutting predictions. For the case of fatigue life, the difference due to local calibrations reached more than 50%, with an average value of 17.33 %. This result agrees with Cooper et al. [19] study, which concluded that the predicted alligator cracking would change by 60 % with changing the dynamic modulus value. In addition, this result agrees with Cheng et al. [20], who concluded that changing the dynamic modulus value in the MEPDG analysis procedure would significantly change the

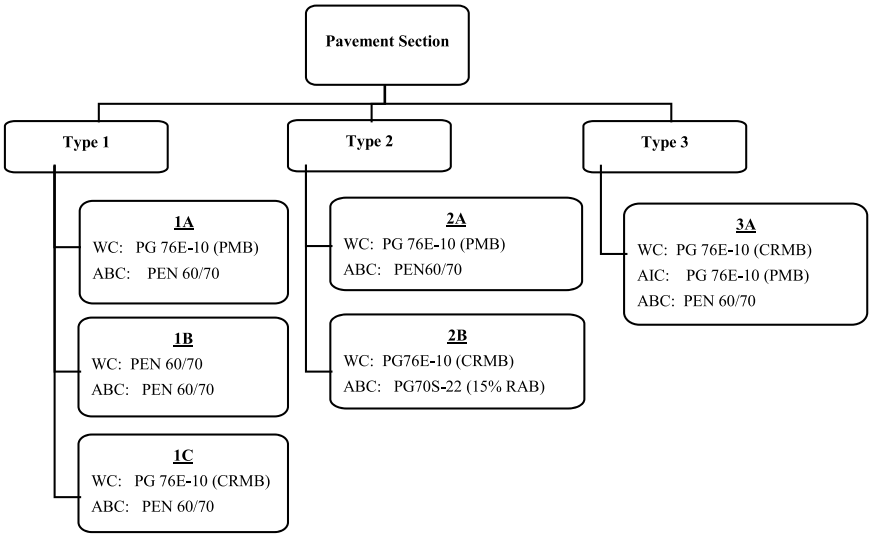

Fig. 7. Binder type matrix for the collected pavement structures.

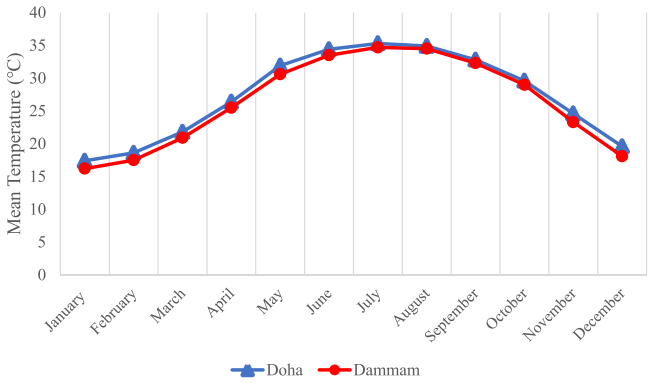

Fig. 8. Mean monthly temperatures for Doha and Dammam cities.

Table 17
Traffic load inputs for ME analysis on the MEAPA website.

Traffic parameter	Pavement structure[a]		
	Type 1	Type 2	Type 3
AADT[b] (veh/day)	220	3344	6672
Lane Factor	1.00	0.90	0.60
Distribution Factor	0.55	0.55	0.55
Speed (kph)	50	60	100
Analysis Period (yrs)	20	20	20

[a] Refer to Figs. 6 and 7 for pavement structures and binder types.
[b] AADT stands for Annual Average Daily Traffic.

predicted field strains. Accordingly, using locally calibrated is required to give more reliable pavement performance prediction and designs.

Despite that R^2 of the Hirsch model prediction performance was improved by around 2 %, which is considered insignificant in another study [8], the new dynamic modulus values have changed the predicted performance of pavement structures. This implements the importance of investigating the practical effect of the calibration in this area.

8. Conclusions

The following conclusions are drawn from the above-mentioned investigation and its findings:

Table 18
Percent change in the fatigue and rutting due to Hirsch model calibration.

Pavement section[a]	Fatigue (m/km)		Percent change (%)	Rutting (cm)		Percent change (%)
Calibration status	Before	After		Before	After	
1A	126.06	157.50	24.94	0.51	0.58	13.73
1B	143.47	224.51	56.49	0.51	0.53	3.92
1C	188.31	180.30	-4.25	0.53	0.53	0.00
2A	662.23	892.19	34.73	0.71	0.79	11.27
2B	870.40	746.44	-14.24	0.71	0.66	-7.04
3A	578.69	615.22	6.31	0.64	0.64	0.00
Average =			**17.33**			**3.65**

[a] Refer to Figs. 6 and 7 for pavement structures and binder types.

- Hirsch model showed high prediction performance for Qatar asphalt mixtures with R^2 value of 87.2 % prior to calibration. Alkhateeb model, however, showed lower performance with an R^2 value of 70.8 %. The calibration improved the R^2 value of the Hirsch and Alkhateeb models to 89.2 % for both.
- The sensitivity analysis showed that the Hirsch and Alkhateeb models had higher performance in PEN60/70 and PG 76E-10 mixtures and lower performance in RAB mixtures.
- While the implemented calibration technique improved the overall performance of both models, more bias was introduced for RAB mixtures in both models after calibration.
- Both uncalibrated Hirsch and Alkhateeb models had a low predictive performance at test temperatures higher than 35 °C, which improved with model calibration.
- Hirsch model showed consistent performance over-tested frequencies between 0.1 and 20 Hz with an R^2 value ranging between 70 % and 90 %. However, the uncalibrated Alkhateeb model showed significant bias at high frequencies.
- The uncalibrated Alkhateeb model showed poor performance at low temperatures of 4–5 °C and a frequency of 10–20 Hz. This performance was improved as a result of the model calibration.
- Mechanistic-Empirical analysis for pavement structures of Qatar showed significant change in the predicated fatigue distress, reaching more than 50 % after considering the calibrated master curve of the asphalt mixtures with an average value of 17.33 %. This result confirmed that using the locally calibrated models will give more reliable pavement performance prediction and designs.
- While the calibration changed the R^2 value of the Hirsch model only by 2 %, there is a significant change in the predicted pavement performance using the MEPDG method. This finding highlights the importance of considering the practical effect of the calibration in this area.

CRediT authorship contribution statement

Ahmad Al-Tawalbeh: Investigation, Formal analysis, Writing – original draft. **Okan Sirin:** Funding acquisition, Conceptualization, Supervision, Writing – review & editing. **Mohammed Sadeq:** Conceptualization, Writing – review & editing. **Haissam Sebaaly:** Data curation, Writing – review & editing. **Eyad Masad:** Funding acquisition, Conceptualization, Supervision, Writing – review & editing.

Declaration of Competing Interest

The authors declare that they have no known competing financial interests or personal relationships that could have appeared to influence the work reported in this paper.

Data Availability

No data was used for the research described in the article.

Acknowledgments

This publication was jointly supported by Qatar University and Texas A&M University at Qatar, IRCC-2019-011 (International Research Collaboration Co-Fund). The findings achieved herein are solely the responsibility of the authors. Qatar National Library funded the open-access publication of this article.

References

[1] American Association of State Highway and Transportation Officials, AASHTO Guide for Design of Pavement Structures, 1993, The Association, Washington, D. C., 1993.
[2] S. El-Badawy, F. Bayomy, A. Awed, Performance of MEPDG dynamic modulus predictive models for asphalt concrete mixtures: local calibration for Idaho, J. Mater. Civ. Eng. 24 (11) (2012) 1412–1421, https://doi.org/10.1061/(asce)mt.1943-5533.0000518.
[3] D.W. Christensen Jr., T. Pellinen, Amon F. Bonaquist, Hirsch model for estimating the modulus of asphalt concrete, Asph. Paving Technol. no. 72 (2003) 97–121.
[4] G. Al-Khateeb, A. Shenoy, N. Gibson, T. Harman, A new simplistic model for dynamic modulus predictions of asphalt paving mixtures, in: Proceedings of the 2006 Annu. Meet. Assoc. Asph. Paving Technol., no. January, 2006.
[5] G.S. Moussa, M. Owais, Pre-trained deep learning for hot-mix asphalt dynamic modulus prediction with laboratory effort reduction, Constr. Build. Mater. 265 (2020), 120239, https://doi.org/10.1016/j.conbuildmat.2020.120239.
[6] G.S. Moussa, M. Owais, Modeling hot-mix asphalt dynamic modulus using deep residual neural networks: parametric and sensitivity analysis study, Constr. Build. Mater. 294 (2021), 123589, https://doi.org/10.1016/j.conbuildmat.2021.123589.
[7] C. Zhang, S. Shen, X. Jia, Modification of the Hirsch dynamic modulus prediction model for asphalt mixtures, J. Mater. Civ. Eng. 29 (12) (2017) 04017241, https://doi.org/10.1061/(asce)mt.1943-5533.0002099.
[8] M.M. Robbins, D.H. Timm, Evaluation of dynamic modulus predictive equations for southeastern United States asphalt mixtures, Transp. Res. Rec. (2210) (2011) 122–129, https://doi.org/10.3141/2210-14.
[9] M. Kang, T.M. Adams, Local calibration for fatigue cracking models used in the mechanistic-empirical pavement design guide, in: Proc. 2007 Mid-Continent Transp. Res. Symp., 2007.
[10] C. Zhang, S. Shen, X. Jia, Modification of the Hirsch dynamic modulus prediction model for asphalt mixtures, J. Mater. Civ. Eng. 29 (12) (2017) 1–8, https://doi.org/10.1061/(ASCE)MT.1943-5533.0002099.
[11] M. Kim, Development of Differential Scheme Micromechanics Modeling Framework for Predictions of Hot-mix Asphalt (HMA) Complex Modulus and Experimental Validations (Ph.D. Diss), Univ. Illinois Urbana, Champaign, IL, 2010.
[12] S. Yousefdoost, B. Vuong, I. Rickards, P. Armstrong, B. Sullivan, Evaluation of dynamic modulus predictive models for typical Australian asphalt mixes, in: Proceedings of the 15th AAPA Int. Flex. Pavements Conf., vol. 19, 2013, pp. 1–18.
[13] M.S.S. Far, B.S. Underwood, S.R. Ranjithan, Y.R. Kim, N. Jackson, Application of artificial neural networks for estimating dynamic modulus of asphalt concrete, Transp. Res. Rec. (2217) (2009) 173–186, https://doi.org/10.3141/2127-20.
[14] J. Li, A. Zofka, I. Yut, Evaluation of dynamic modulus of typical asphalt mixtures in Northeast US Region, Road Mater. Pavement Des. 13 (2) (2012) 249–265, https://doi.org/10.1080/14680629.2012.666641.
[15] N. Solatifar, Performance evaluation of dynamic modulus predictive models for asphalt mixtures, J. Rehabil. Civ. Eng. 8–3 (2020) 87–97, https://doi.org/10.22075/JRCE.2020.17391.1324.
[16] S. Shen, H. Yu, K.A. Willoughby, J.R. Devol, J.S. Uhlmeyer, Local practice of assessing dynamic modulus properties for Washington state mixtures, Transp. Res. Rec. 2373 (2373) (2013) 89–99, https://doi.org/10.3141/2373-10.
[17] A.M. Khattab, S.M. El-badawy, A. Abbas, A. Hazmi, M. Elmwafi, Evaluation of Witczak E* predictive models for the implementation of AASHTOWare-Pavement ME Design in the Kingdom of Saudi Arabia, Constr. Build. Mater. 64 (August) (2014) 360–369, https://doi.org/10.1016/j.conbuildmat.2014.04.066.
[18] S. El-Badawy, R. Abd El-Hakim, A. Awed, Comparing artificial neural networks with regression models for hot-mix asphalt dynamic modulus Prediction, J. Mater. Civ. Eng. 30 (7) (2018) 04018128, https://doi.org/10.1061/(asce)mt.1943-5533.0002282.
[19] S.B. Cooper, L.N. Mohammad, M.A. Elseifi, A. Raghavendra, Dynamic modulus of asphalt mixtures: evaluation of effects on pavement performance prediction, Transp. Res. Rec. 2507 (2015) 67–77, https://doi.org/10.3141/2507-08.
[20] H. Cheng, Y. Wang, L. Liu, L. Sun, Effects of using different dynamic moduli on predicted asphalt pavement responses in mechanistic pavement design, Road Mater. Pavement Des. (May) (2021), https://doi.org/10.1080/14680629.2021.1924842.
[21] Ministry of Transport & Communication, Qatar Highway Design Manual, The Ministry, Doha, 2015.
[22] Public Work Authority, PWA Interim Advice Note No. 101 Rev 2, The Public Work Authority, Doha, 2016.
[23] M. Witczak, Simple Performance Tests: Summary of Recommended Methods and Database, Washington, D.C., 2006. ⟨https://doi.org/10.17226/13949⟩.
[24] Q.M. Department, Qatar Climatological Normals. ⟨https://qweather.gov.qa/CAA/ClimateNormals.aspx⟩, (Accessed 15 November 2020).
[25] Q.M. Department, Qatar Climatological Normals. ⟨https://qweather.gov.qa/CAA/ClimateNormals.aspx⟩, (Accessed 14 November 2021).
[26] American Association of State Highway and Transportation Officials, Standard Practice for Developing Dynamic Modulus Master Curves for Asphalt Mixtures using the Asphalt Mixture Performance Tester (AMPT). Washington, DC, 2017.
[27] L.K. Roja, E. Masad, W. Mogawer, Performance and blending evaluation of asphalt mixtures containing reclaimed asphalt pavement, Road Mater. Pavement Des. 22 (11) (2021) 2441–2457.
[28] L.K. Roja, M.F. Aljarrah, O. Sirin, N. Al-Nuaimi, E. Masad, Rheological, thermal, and chemical evaluation of asphalt binders modified using crumb rubber and warm-mix additive, J. Mater. Civ. Eng. 34 (5) (2022) 04022049.
[29] H. Sebaaly, P.P. Riviera, S. Varma, J.W. Maina, E. Santagata, Performance-based assessment of rutting resistance of asphalt mixes designed for hot climate regions, Int. J. Pavement Eng. (2020) 1–12, https://doi.org/10.1080/10298436.2020.1858484.
[30] M. of Environment. Qatar Construction Specification 2014, 2nd ed., The Ministry, Doha, 2014.
[31] T. Pellinen, Kristiina, Investigation of the Use of Dynamic Modulus as an Indicator of Hot-mix Asphalt Performance, Arizona State Univ., vol. Thesis (PH, 2001.
[32] S. Cano-Ortiz, P. Pascual-Muñoz, D. Castro-Fresno, Machine learning algorithms for monitoring pavement performance, Autom. Constr. 139 (May) (2022), 104309, https://doi.org/10.1016/j.autcon.2022.104309.
[33] M.E. Kutay, M. Lanotte, Formulations of the Pavement Performance Prediction Models in the Mechanistic-Empirical Asphalt Pavement Analysis (MEAPA) Web Application, 2020, [Online]. Available: ⟨https://paveapps.com/meapaapp2/⟩.
[34] National Cooperative Highway Research Program, Guide for Mechanistic–Empirical Design of New and Rehabilitated Pavement Structures (Final Report), Transportation Research Program, National Research Council, Washington DC, 2004.
[35] N.C. for Meteorology, KSA Climatological Normals. ⟨www.ncm.gov.sa⟩, (Accessed 29 April 2022).